Available online at www.sciencedirect.com
SCIENCE DIRECT®
International Journal of Heat and Mass Transfer 47 (2004) 4569–4577
International Journal of HEAT and MASS TRANSFER
www.elsevier.com/locate/ijhmt

Effects of non-isothermal heating on drag reduction in surfactant aqueous solution flow

Kimitoshi Sato [a], Noriyuki Furuichi [b,*], Naoki Matsumoto [b], Masaya Kumada [b]

[a] *Department of Mechanical System Engineering, Hiroshima Institute of Technology, 2-1-1, Miyake, Hiroshima, Saeki-ku 731-5193, Japan*

[b] *Department of Mechanical and Systems Engineering, Faculty of Engineering, Gifu University, 1-1, Gifu, Yanagido 501-1193, Japan*

Received 20 May 2003
Available online 5 June 2004

Abstract

In this study we investigate the control of flow characteristics and heat transfer of a drag-reducing dilute cationic surfactant solution in a channel, in order to develop a highly efficient heat exchanger. As has been reported by many authors, addition of certain polymers or surfactants reduces heat transfer in drag-reduced water flow. Therefore, other measures must be taken in order to compensate the reduction in heat transfer. Specifically, this study investigates the effects of non-isothermal heating on drag-reduced flow: experiments were conducted in order to study passive control for effecting the drag-reduction state by employing temperature-dependent physical properties and heat transfer augmentation by complex flow. In addition, velocity and temperature profiles were measured under the coexistence of turbulent and drag-reducing flow in order to clarify the effect of drag reduction. It was confirmed that the drag reduction state was changed and diminished due to the temperature rise near the wall, especially the condition in the region of $50 < y^+ < 100$ greatly influence on drag reduction of pipe flow.

1. Introduction

Adding a small amount of surfactant to water is effective for reducing the pressure loss of fluid transportation in pipes and channels. This phenomenon is due to reduction of turbulent frictional drag, and has been regarded noteworthy since its discovery [1]. Investigations of this effect have been summarized by Hoyt [2], Virk [3], Ohendolf et al. [4] and Gyr and Bewersdorff [5]. Unfortunately many investigators have reported that heat transfer is reduced simultaneously in the drug-reducing flow [6–8]. Successful application of this phenomenon to development of a highly efficient heat exchanger requires advanced technology for heat transfer augmentation.

In an effort to compensate for reduced heat transfer, several ways of modification of heat transfer surface have been studied [9–11]. The authors had examined the effect of several turbulent promoters: a two-dimensional fence, triangle ribs and delta wings in the previous studies [12,13]. In these experimental investigations, a large effect of drag reduction was realized as in the case of the plane channel. In the drag-reducing flow, the two-dimensional fence showed greater effectiveness in increasing net heat transfer than did the row of delta wings. However, delta winglets showed higher efficiency of heat transfer in drag-reducing flow than did the plane channel and the channel with the two-dimensional fence, because of the small pressure drop and restoration of the streamwise degradation of heat transfer. Particularly, delta wings that create longitudinal vortex increased the heat transfer coefficient over the test section for both the water and surfactant flow.

This heat transfer enhancement technique can be considered a passive measure using intricate turbulent

* Corresponding author. Tel.: +81-58-293-2538; fax: +81-58-230-1892.
E-mail address: furuichi@cc.gifu-u.ac.jp (N. Furuichi).

0017-9310/$ - see front matter © 2004 Elsevier Ltd. All rights reserved.
doi:10.1016/j.ijheatmasstransfer.2003.08.029

Nomenclature

H	height of channel [m]
h	heat transfer coefficient [W/m^{2}K]
k	thermal conductivity [W/mK]
Nu	Nusselt number
Re	Reynolds number
u'	root mean square of turbulent velocity fluctuation in the streamwise direction [m/s]
U	streamwise velocity [m/s]
x	downstream distance from the leading edge of heat transfer section [m]
y	wall distance from heating surface in normal direction [m]
λ	friction factor
υ	kinematic viscosity [m^2/s]

Subscripts and superscripts

b	bulk
m	mean
w	wall
+	normalized by wall unit

promoting facilities, which require precise manufacturing technology and therefore increased production cost. Moreover, the surfactant solution flow shows the characteristics of non-Newtonian fluid which depend on fluid temperature[14,15]. Particularly, Kawaguchi and coworkers reported the temperature dependency in shear viscosity of the surfactant solution which was the same one used in this study: the apparent viscosity decreased sharply and showed the value of water when the fluid temperature exceeded a critical point [16,17]. Meanwhile, the following are known: (1) frictional drag in surfactant aqueous solution flow is much lower than that in water; (2) when fluid temperature (bulk) rises, drag-reducing flow changes back to turbulent, like water flow. In consideration of these facts, our objective is to solve the problem in understanding the phenomenon of drag reduction: "Which is the dominant factor for the net drag reduction in pipe flow, the condition of all flow including the free stream, or the condition of only the flow near the wall?" In order to clarify the mechanism of drag reduction and achieve higher efficiency of heat transfer with simple equipment, in this study heat flux on the wall surface was varied in order to change the condition in developed drag-reducing flow from the viewpoint of the temperature dependency of fluid properties; specifically, the effects of the presence and absence of drag reduction were examined. The objective of our study is to clarify at which location temperature should be changed in order to contribute to drag reduction, by effecting wall heating so as to arrange a vertically and longitudinally "non-isothermal field" in channel flow.

2. Experimental setup and procedures

The experiments were carried out in a closed loop flow channel consisting of a reservoir tank, a centrifugal pump, an inlet chamber, a nozzle, a test section, a diffuser, an outlet chamber and a flow meter, as shown in Fig. 1. A two-dimensional channel (PMMA; 10 mm height, 125 mm width, and 3500 mm length) was adopted as the test section. The pressure drop in the axial direction was measured at 12 points located on the test channel at 125 mm intervals, by use of a 0.5 mm plastic pipe connection to a diaphragm-type pressure

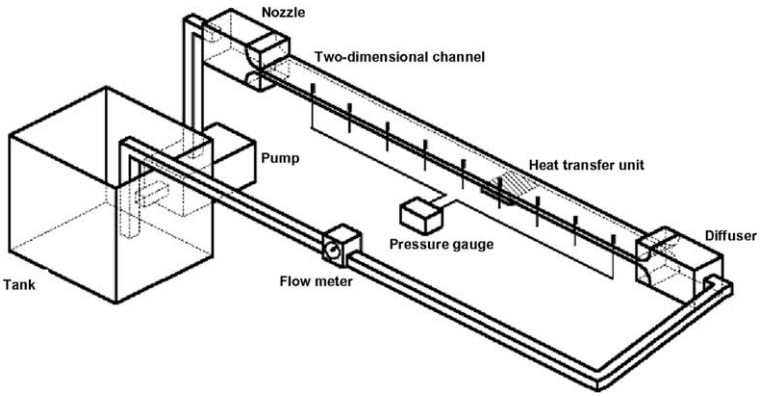

Fig. 1. Closed-loop two-dimensional water channel.

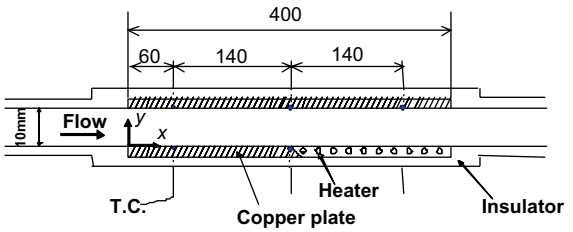

Fig. 2. Schematic diagram of heat transfer test section.

transducer and via a pressure amplifier, and output was recorded in a digital voltmeter and data logger. The direction of main flow, the vertical direction, and the span direction are defined as the X, Y, and Z axes, respectively.

The heating section is located 2.25 m downstream from the entrance of the channel. Fig. 2 shows the details of the heat transfer experimental unit. Two copper plates in opposition to each other were embedded in the upper and lower walls of the channel. They were heated independently by use of 40 rod heaters, which were controlled with an electric current from a stabilized DC power source (maximum heat flux: 64 kW/m^2). The temperature at the wall surface was maintained within the deviation of ±0.1 °C using three thermocouples embedded in the heating plates on the center line of the channel as shown in Fig. 2.

The cationic surfactant used in this study was cetyltrimethyl ammonium chloride (CTAC), which was added to tap water in equal weight with sodium salicylate serving as a counter ion. The tested fluid was controlled to maintain a constant temperature of 40 °C by the heater and the cooler installed in the tank.

Velocity measurement was carried out by multi-point Laser Doppler Velocimetry (LDV) [18]. Fig. 3 shows an optical system of the advanced multi-point LDV. This LDV is made very compact, by virtue of employing a semiconductor laser with a maximum power of 40 mW and a wavelength of 685 nm, and an optical fiber unit with 96 plastic fibers having a diameter of 0.25 mm.

The sampling frequency of raw data is 2 MHz, and the sampling interval of the velocity data is 0.128 ms so as to enable frequency analysis by FFT of 256 points. Therefore, the data-sampling rate is about 7812/s. The sampling time length for one run is set to about 8 s. In this experiment, the rate of capture for the velocity data is maintained at 70% or more. Therefore, the velocity and turbulence intensity were computed from an average of 43750 data points. The spatial resolution of each measuring point established in the X–Z plate is 0.22–1.40 mm, as determined by the cross angle of the laser light sheet, and the resolution in the Y direction is 0.24 mm, which corresponds to the core diameter of the receiving optical fiber. With regard to seeding, polystyrene particles having a mean diameter of 5 μm were used as tracer particles for measurement of velocity.

Fig. 4 shows a thermocouple probe for measurement of temperature profile (K-type, ϕ 0.1 mm). A thermocouple junction was held by a support rod. In order to insert this rod into the flow, the upper-side wall has eight holes at intervals of 8 mm. The thermocouple probe was traversed in the Y-direction by use of a micro traverser.

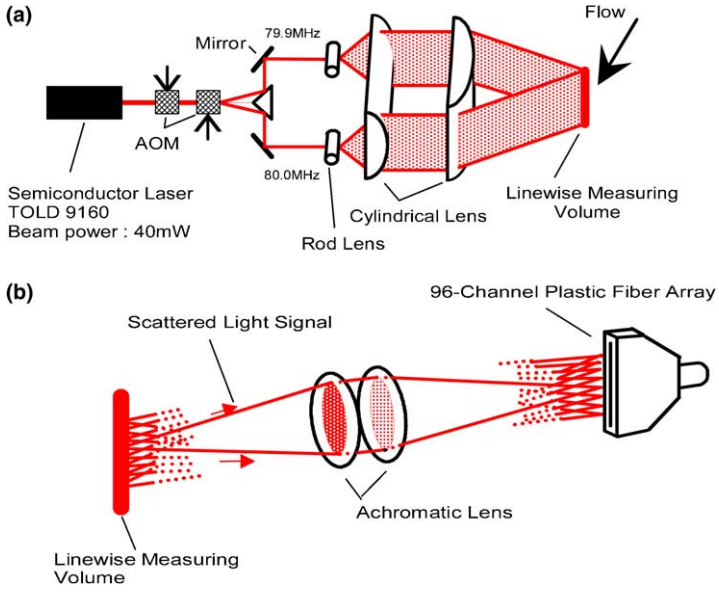

Fig. 3. LDV measurement system (a) transmitting optics (b) receiving optics.

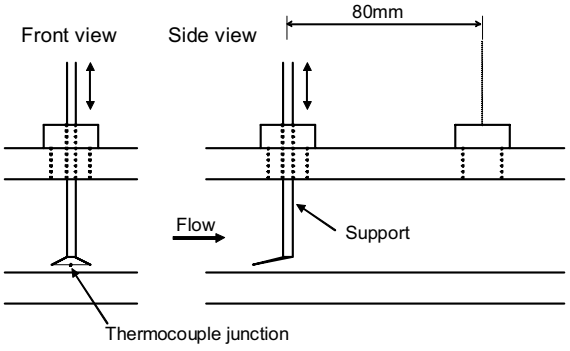

Fig. 4. Thermocouple probe.

3. Results and discussion

3.1. Friction factor and heat transfer coefficient

In order to examine the drag reduction effect, the pressure loss in the test channel was measured while wall temperature was controlled at some flow velocities. The conditions of wall heating are $T_w = 44$, 46, 48 °C. Example results (at $Re = 2.5 \times 10^4$) are shown in Fig. 5. The local pressure in the heat transfer test section is unknown, because static holes had not been drilled in the heating plates. Therefore, the extrapolated pressure gradient is drawn in broken lines in the figure. In the case of 50 ppm surfactant solution, turbulence was not recovered to a great extent when T_w was set to 44 °C. However, when bulk temperature was set to 44 °C, the condition of drag-reduced flow becomes almost identical with that of water flow.

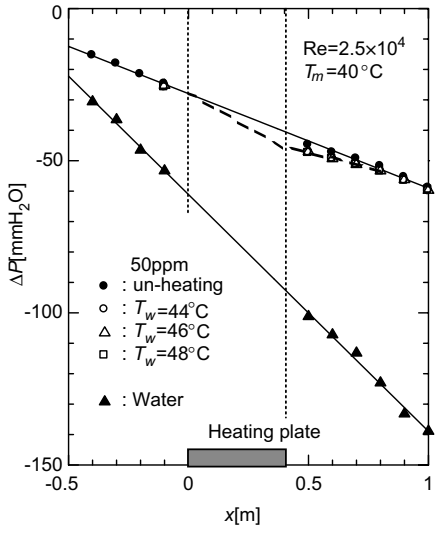

Fig. 5. Pressure drops of surfactant solution flow.

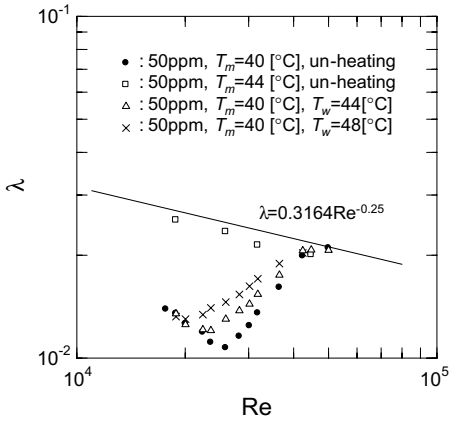

Fig. 6. Relationship between friction factor and Reynolds number.

Fig. 6 shows friction factor vs. Reynolds number for surfactant solution (CTAC 50 ppm) in a channel flow. The fluids were maintained at 40 degrC. Reynolds number is defined as $Re = UH/\upsilon$, where υ is kinematic viscosity of water. The figure also shows the Blasiuss's equation representing the characteristics of water flow. In the case of surfactant solution flow, the extrapolated pressure loss gradient was used for calculation of friction factor.

In the case of $T_w = T_m = 40$ °C, friction factor decreases with increasing Reynolds number up to a certain point, and its maximum drag reduction reaches 75% that of water. When Reynolds number is increased further, the friction factor increases and rapidly approaches that of water. Using this value as a boundary, we identified two flow regions: a fully drag-reducing region and a recovery region.

The authors have reported the effects of the concentration and flow rate on drag reduction and heat transfer in the previous study. It was confirmed that the low-density solution of tens ppm is effective on the heat transfer at the conditions of Reynolds number at around the critical point of drag reduction. In this study the change in flow pattern in this region is remarked.

The influence of bulk temperature on drag reduction was compared with that of wall temperature. In the case of $T_w = T_m = 40$ °C, the friction factor is almost equal with that of water. However, the friction factor increased with wall temperature; that is, $T_w = 44$ and 48 °C yielded different results.

The effect of wall heating on drag reduction was investigated. Fig. 7 shows the relationship between friction factor and wall temperature for water and a surfactant solution (CTAC 50 ppm) in a channel flow at $Re = 2.5 \times 10^4$ at 40 °C. In the case of surfactant solution flow at $T_w = 40$ °C, drag reduction reached 56%.

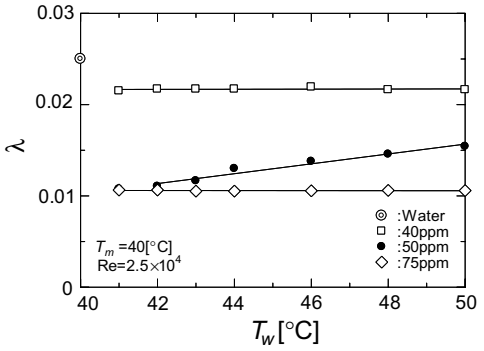

Fig. 7. Influence of wall heating on frictional drag of surfactant solution flow.

Friction factor of the surfactant flow increased with wall temperature and approached that of water flow.

The heat transfer tests were carried out at $Re = 2.5 \times 10^4$ in a manner similar to that of the frictional drag tests. The tested fluids were 40, 50, and 75 ppm CTAC solutions and water. Wall temperature was controlled by adjusting heat flux, and was set at 40, 44, 46, 48, and 50 °C.

Fig. 8 shows the relationship between Nusselt number and wall temperature. Nusselt number is defined as $Nu = hH/k$, where k is the thermal conductivity of water. In the cases of 40 and 75 ppm surfactant aqueous solution, wall heating had no observed effect on Nu. In contrast, in the case of 50 ppm surfactant aqueous solution, Nu increased with temperature. Therefore, the quantity of friction factor; namely, the presence or absence of the drag reduction phenomenon, was observed to be proportional to the degree of heat transfer.

The above results indicate that changing the wall heat flux to the fluid to control the wall temperature beyond the critical temperature of drag reduction elimination dynamically influenced the flow field and heat transfer.

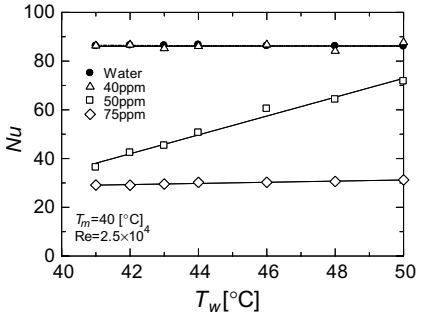

Fig. 8. Influence of wall heating on heat transfer of surfactant solution flow.

3.2. Velocity and temperature profiles

In this experimental study, no exact information about the local frictional drag within the heating section was available. Therefore, the influence of non-isothermal heating on drag reduction was examined by use of velocity profiles by LDV measurement at local points in the flow direction in the channel.

The tested fluids were 50 ppm CTAC solution and water. Fluid temperature was 40 °C and Reynolds number was set at 2.5×10^4 and 3.2×10^4, the former for the point of largest drag reduction and the latter for the recovery region. Wall temperature was set at 40, 44, 46, and 48 °C.

Fig. 9(a) shows mean velocity profiles normalized by the inner layer scale at $x/(H/2) = 64$ in the case of $Re = 2.5 \times 10^4$. The two solid lines in Fig. 9(a) respectively represent the viscous sublayer

$$u^+ = y^+ \tag{1}$$

and the boundary layer near the wall, assuming a Newtonian fluid.

$$u^+ = 2.5 \ln y^+ + 5.5 \tag{2}$$

As seen in the figure, the water profile complies with the Newtonian profile, and the surfactant solution profile for $T_w = T_m = 40$ °C is approximately semilogarithmic with a slope 12, which is shifted downward from but parallel to the Virk's ultimate profile [3].

$$u^+ = 11.7 \ln y^+ - 17.0 \tag{3}$$

This profile shows a buffer layer which is thicker than the one represented by Eqs. (1) and (3) (the heavy, solid and broken line in Fig. 9(a), respectively).

In the case of $T_w = 44$ °C, in contrast with the fully drag-reduced flow, the velocity profile is parallel to the Newtonian law of the wall at $y^+ < 50$, and the profile of drag-reducing flow reappears at $y^+ > 50$. Furthermore, the profile for $T_w = 46$ °C shows an upward shift from the profile for $T_w = 44$ °C, but at $y^+ > 100$, profile exhibits a slope of the Newtonian profile for the wall. In case of $T_w = 48$ °C, the entire profile is parallel to the Newtonian profile. These results indicate that the condition in the region of $50 < y^+ < 100$ greatly influences drag reduction of pipe flow. Fig. 9(b) shows turbulent intensity profiles. The u' components in cases of wall heating also increase with wall temperature.

Velocity and turbulence intensity profiles for 50 ppm CTAC solution flow of $Re = 2.5 \times 10^4$ at the local points in flow direction at the heating section and its downstream are shown in Fig. 10(a) and (b) for $T_w = 44$ °C and in Fig. 11(a) and (b) for $T_w = 48$ °C. As shown in Figs. 10(a) and 11(a), in each case the effect of heating on the flow appears after the center of the heating surface.

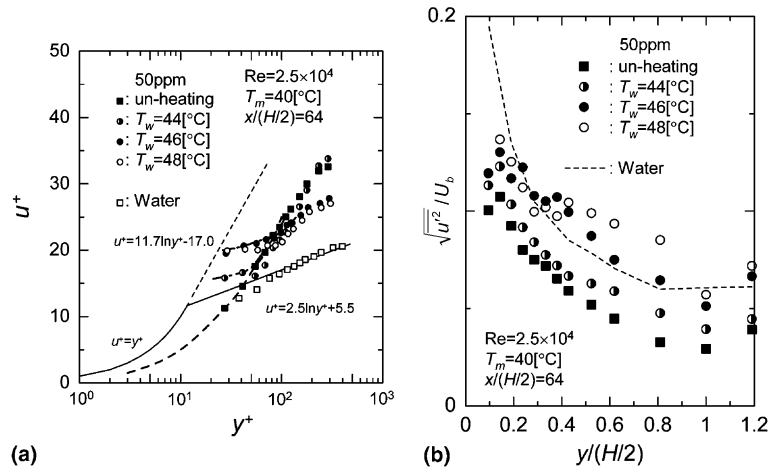

Fig. 9. Variations of the velocity and turbulent intensity profiles respect to wall temperature ($x/(H/2) = 64$).

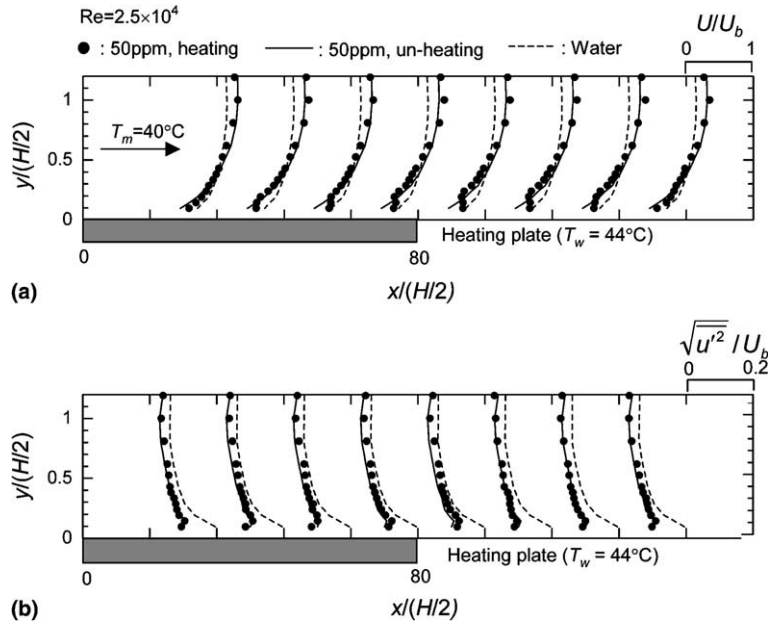

Fig. 10. Streamwise variation of velocity and turbulent intensity profile (50 ppm, $T_w = 44$ °C, $Re = 2.5 \times 10^4$).

The flow accelerates; as a result, the velocity profiles near the wall show steep gradients. However, the accelerated layer is thicker in the case of $T_w = 48$ °C; that is, at $y/(H/2) = 0.1$–0.3. The difference in velocity profiles of main flow between the cases of $T_w = 44$ °C and 48 °C is observed instead. The result in case of $T_w = 44$ °C is distributed along the profile for drag reducing flow and that in case of $T_w = 48$ °C shows one for water. Further, the flat velocity gradient is confirmed to appear near the wall surface, within $y/(H/2) < 0.2$; $y^+ < 50$, as a result of wall heating, and this effect is not observed in the case of the flow in the recovery region.

Frictional drag increases with fluid temperature rise near the wall, and subsequently the flow returns to the developing condition. As the fluid runs downstream it returns to the condition before wall heating, but changes slowly in the case of $T_w = 48$ °C.

As shown in Fig. 11(b), in the case of $T_w = 48$ °C at $x/(H/2) = 80$, turbulence intensity also increases over the entire sectional region; nevertheless, turbulence

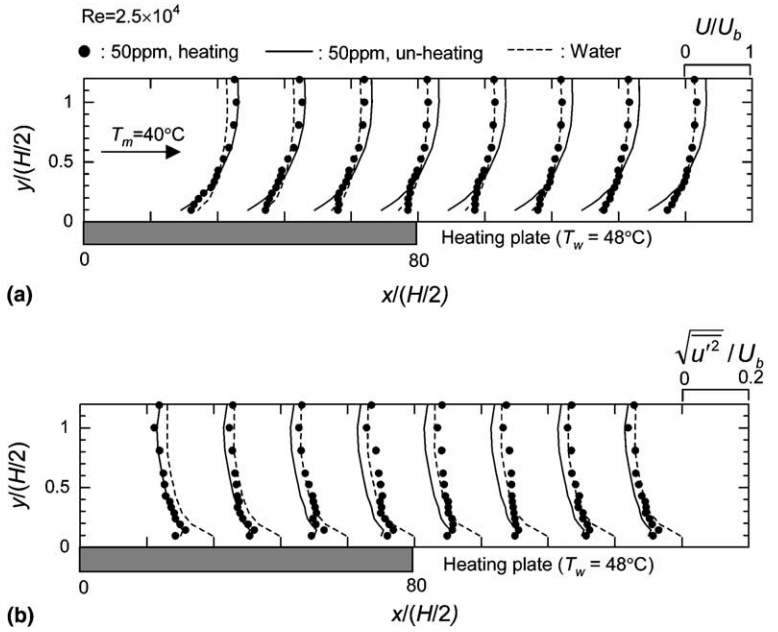

Fig. 11. Streamwise variation of velocity and turbulent intensity profile (50 ppm, $T_w = 48$ °C, $Re = 2.5 \times 10^4$).

intensity near the wall is insignificant. When the fluid is not heated after the heating section, the turbulence near the wall decreases. Turbulent characteristic is considered to show different temperature dependence in main flow and near the wall, because recovery of bulk friction factor does not appear strongly in the case of wall heating, although it shows the flow pattern for water in main flow.

Velocity and turbulence intensity profiles for 50 ppm CTAC solution flow of $Re = 3.2 \times 10^4$ are shown

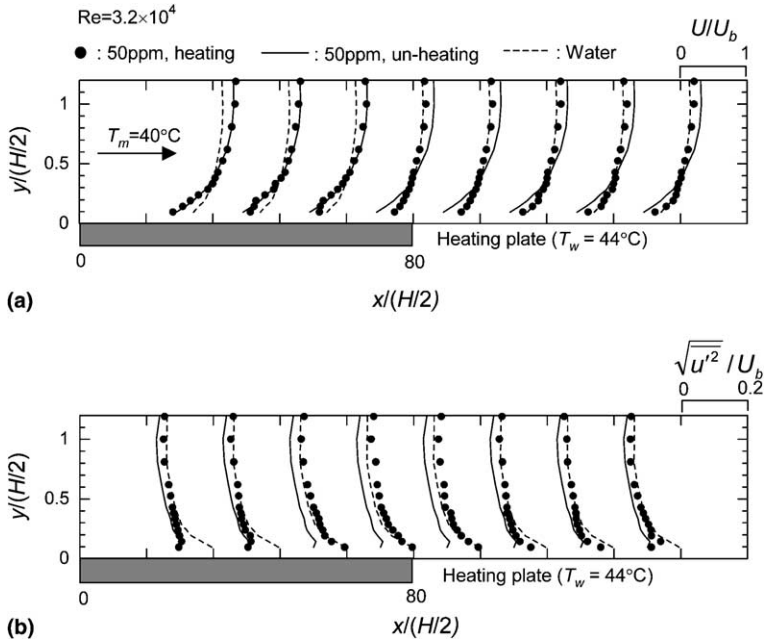

Fig. 12. Streamwise variation of velocity and turbulent intensity profile (50 ppm, $T_w = 44$ °C, $Re = 3.2 \times 10^4$).

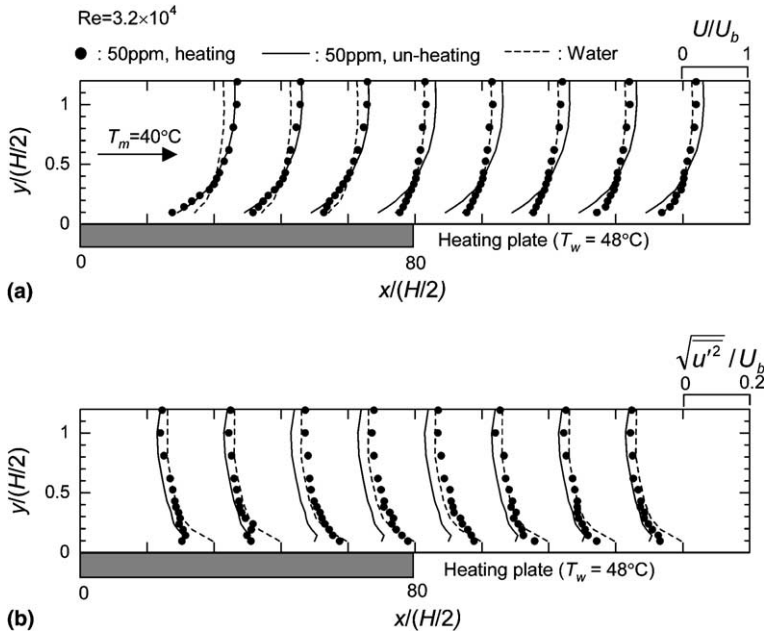

Fig. 13. Streamwise variation of velocity and turbulent intensity profile (50 ppm, $T_w = 44$ °C, $Re = 3.2 \times 10^4$).

in Fig. 12(a) and (b) for $T_w = 44$ °C and in Fig. 13(a) and (b) for $T_w = 48$ °C. The point of observation is considered to fall in the recovery region of turbulence for each wall temperature. Therefore, in each case velocity and turbulence intensity profiles become similar to those of water flow after the heating section until the downstream end. The S-line velocity profiles observed in the case of $Re = 2.5 \times 10^4$ do not appear in this condition.

Temperature profiles were measured for drag-reducing and drag-recovered flow. The experimental conditions were similar to those employed in velocity profile measurement. The experiments were carried out under the condition of the prescribed surface temperature.

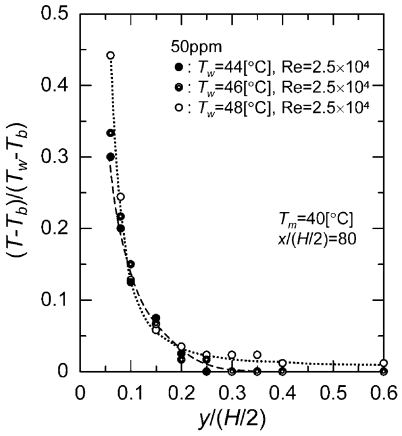

Fig. 14. Variations of temperature profiles respect to wall temperature ($x/(H/2) = 80$).

Fig. 14 shows temperature profiles of surfactant solution flows in the cases of $T_w = 44$, 46 and 48 °C at $x/(H/2) = 80$. The profiles for $T_w = 44$ and 46 °C intersect the profile for $T_w = 48$ °C at $y/(H/2) = 0.2$; namely $y^+ = 50$. If flow condition is held constant, such intersection in the profile cannot exist. Kawaguchi et al. reported the existence of double layers, which show different diffusivity under measurement of temperature profiles near the heating wall [19]. According to that study, the outer layer prevents diffusion out to the main flow. The aspect of the flat temperature profiles near the wall in the case of wall heating at $Re = 2.5 \times 10^4$ indicates the existence of these layers. Furthermore, the crossed profiles as seen in Fig. 14 suggest that the outer layer is thinned.

4. Conclusion

Characteristics of drag and heat transfer of dilute surfactant aqueous solution flow in an non-isothermal field were investigated in order to clarify the mechanism of drag reduction and its temperature dependency. The results confirmed that the drag reduction state was diminished and heat transfer was promoted by controlling heat flux on the heating wall and the change in fluid characteristics with temperature.

Turbulence characteristics and temperature profiles have been measured by an LDV system and a fine thermocouple probe. A difference in main flow velocity profiles between the cases of $T_w = 44$ and 48 °C has been observed: the former is distributed along the profile for drag-reducing flow, and the latter is similar to that for water as turbulent flow. The results also confirm that the flat velocity gradient appears near the wall surface under wall heating, which is not observed in the cases of flows in the recovery region of turbulence. Investigation of the effect of non-isothermal heating on drag-reducing flow revealed that the temperature dependent condition of flow and temperature field in the layer near the wall (less than $y^+ = 50$) is an important factor for controlling heat transfer in the drag-reducing flow.

References

[1] B.A. Toms, Some observations on the flow of linear polymer solutions through straight tubes at large Reynolds numbers, in: Proc. First Int. Cong. Rheol. 2 (1948) 135–141.

[2] J.W. Hoyt, The effect of additives on fluid friction, ASME J. Basic Eng. 94 (1972) 258–285.

[3] P.S. Virk, Drag reduction fundamentals, AIChE J. 21 (4) (1975) 625–656.

[4] D. Ohlendorf, W. Interthal, H. Hohhman, Surfactant systems for drag reduction: physiochemical properties and rheological behavior, Rheol. Acta 25 (1986) 468–486.

[5] A. Gyr, H.W. Bewersdorff, Drag reduction of turbulent flows by additives, Kluwer Academic Publications, 1995.

[6] E.F. Matthys, Some recent developments in conductive heat transfer to drug-reducing fluids, Drag reduction in fluid flow, Techniques for friction control, Paper 6(1), in: Proc. of Int. Conf. of Drag Reduction in Fluid Flow (1989) 129–140.

[7] A. Steiff, K. Klopper, Application of drag-reducing additives in district heating systems, in: Fluid Division Conf., Summer Meeting 1996, ASME, FED-237 (1996) 235–242.

[8] K. Gasljevic, E.F. Matthys, Experimental investigation of thermal and hydrodynamic development regions for drag-reducing surfactant solutions, ASME J. Heat Transfer 119 (1997) 80–88.

[9] M. Fossa, L.A. Tagliafico, Experimental heat transfer of drag-reducing polymer solutions in enhanced surface heat exchangers, Exp. Therm. Fluid Sci. 10 (1995) 221–228.

[10] P. Li, Y. Kawaguchi, H. Daisaka, A. Yabe, K. Hishida, M. Maeda, Heat transfer enhancement to the drag-reducing flow of surfactant solution in two-dimensional channel with mesh-screen inserts at inlet, ASME J. Heat Transfer 123 (2001) 779–789.

[11] Y. Qi, Y. Kawaguchi, Z. Lin, M. Ewing, R.N. Christensen, J.L. Zakin, Enhanced heat transfer of drag reducing surfactant solutions with fluted tube-in-tube heat exchanger, Int. J. Heat Mass Transfer 44 (2001) 1495–1505.

[12] K. Sato, J. Mimatsu, M. Kumada, Drag reduction and heat transfer augmentation of surfactant additives in two-dimensional channel flow, in: Proc. of the Fifth ASME/JSME Joint Therm. Eng. Conf. (1999) AJTE99-6452.

[13] K. Sato, J. Mimatsu, M. Kumada, Turbulent characteristics and heat transfer augmentation of drag reducing surfactant solution flow, Therm. Sci. Eng. 7 (1) (1999) 41–50.

[14] P. Komrzy, K. Svejkovsky, J. Pollert, B. Lu, J.L. Zakin, Drag reduction and heat transfer of cationic surfactant solutions, in: Proc. of ASME 1996 Fluid Eng. Div. Conf., FED, vol. 236 (1996) 31–36.

[15] Y. Hu, E.F. Matthys, Evaluation of micellar overlapping parameters for a drag-reducing cationic surfactant system: light scattering and viscometry, Langmuir 13 (1997) 4995–5000.

[16] Y. Kawaguchi, Y. Tawaraya, M. Tanaka, Viscosity measurements of CTAC: NASal/W micelle solution—temperature effect and wall effect of viscometer, J. Mech. Eng. Laboratory 49 (7) (1995) 12–21, in Japanese.

[17] Y. Kawaguchi, Y. Tawaraya, A. Yabe, K. Hishida, M. Maeda, Active control of turbulent drag reduction in surfactant solutions by wall heating, in: Proc. of ASME 1996 Fluid Eng. Div. Conf., FED, vol. 236 (1996) 47–52.

[18] T. Hachiga, N. Furuichi, J. Mimatsu, K. Hishida, M. Kumada, Development of a multi-point LDV using semiconductor with FFT-based multi-channel signal processing, Exp. Fluids 24 (1998) 70–76.

[19] Y. Kawaguchi, Y. Tawaraya, A. Yabe, K. Hishida, M. Maeda, Existence of double diffusivity fluid layers and heat transfer characteristics in drag-reducing channel flow, in: Proc. Second International Symposium on Turbulence, Heat and Mass Transfer (1997) 157–166.